

Reliability of High-Voltage Tantalum Polymer Capacitors

Erik Reed, George Haddox

KEMET Electronics Corporation, 2835 KEMET Way, Simpsonville, SC 29681

Phone: +1-864-963-6300, Fax: +1-864-228-4081

e-mail: erikreed@kemet.com

Abstract

Tantalum polymer capacitors provide lower ESR and frequently better reliability than conventional MnO₂-based tantalum capacitors. Their lower ESR facilitates significant penetration into challenging low-voltage applications such as CPU decoupling in laptop computers. Success in low-voltage applications was fortunate because at first it proved difficult to fabricate reliable devices with ratings above roughly 16V. Now, new tantalum polymer capacitors exist with ratings of 25V, 35V, and higher that have reliability on par with their lower-voltage siblings.

About seven years ago, time-to-failure data were presented at CARTS that demonstrated the good reliability of 6V tantalum polymer capacitors of aggressive design. Also presented were models for voltage and temperature acceleration that allow customers to estimate lifetime at application conditions based on lifetests performed at accelerated conditions.

The present work pertains to higher-voltage tantalum polymer capacitors with 25-50V ratings. A brief description of the technology that allows higher voltage operation is provided. Time-to-failure data are presented that were collected over a wide range of voltages and temperatures. Trends in the data are identified and models for voltage and temperature acceleration are presented. Finally, typical lifetimes at rated conditions are estimated and are compared with the results originally presented for the 6V capacitors.

Introduction

The first solid tantalum capacitors were manufactured using manganese dioxide (MnO₂) as the cathode layer. MnO₂ decomposition at elevated temperatures provided a “self-healing” mechanism that allows successful manufacture of high-reliability capacitors even though the tantalum pentoxide (Ta₂O₅) dielectric itself is imperfect. The nature of the self healing is that localized heating at defect sites from concentrated leakage current renders the adjacent MnO₂ only slightly conducting, effectively isolating the defective spot in the dielectric from the rest of the capacitor.

MnO₂-based solid tantalum capacitors have been unquestionably successful, but they are not perfect. One of their weaknesses results from the limited electrical conductivity of the MnO₂ cathode material which causes elevated equivalent series resistance (ESR) in the finished capacitor.

Many applications, such as decoupling low-voltage microprocessors, require capacitors with very low ESR¹. The demand for lower ESR contributed to the development of higher conductivity cathode materials, including conducting polymers. Tantalum capacitors made with conducting polymer have ESR that is typically lower by a factor of 2 to 3 than similar capacitors made with MnO₂.

But with introduction of a new cathode material came questions regarding reliability. In response, a study was performed to quantify the reliability of low-voltage tantalum polymer capacitors of very aggressive design made with poly(3,4-ethylenedioxythiophene) (PEDOT) polymer oxidized with iron (III) toluene sulfonate. This process produces PEDOT doped with toluene sulfonate and residual traces of iron. Accelerated time-to-failure lifetests were performed on large samples of these capacitors at various voltages and temperatures and the resulting data were analyzed to determine acceleration factors related to changing voltage and temperature².

These acceleration factors were fit to a pre-existing empirical model to predict median lifespan at any temperature and voltage of interest, and it was found that the median life of these 6V tantalum polymer capacitors might be as long as 1000 years at 85°C and rated voltage -- an entirely satisfactory result. Subsequent work focused on fitting the original data to a physics-based model and demonstrating similar satisfactory performance of 4V and 2.5V devices³.

But, as always, there was a fly in the ointment. It proved reasonably straightforward to extend the initial success to 10V devices, but it was somewhat harder to make reliable 16V devices. Reliable 25V devices remained an elusive goal for many years and much effort was applied to understanding the limitations of the technology.

A significant breakthrough occurred with the arrival of pre-polymerized PEDOT conductive polymer dispersions doped with polystyrene sulfonate that can be used for some or all of the cathode layer in tantalum capacitors⁴. This new technology makes it possible to manufacture reliable tantalum capacitors having much higher rated voltage.

Once again the problem is to prove that the devices are reliable, a problem that is the motivation for the work presented here. The strategy employed here is essentially the same as was previously employed. Large samples of capacitors are lifetested at many temperatures and voltages, and time-to-failure (TTF) data are collected using an apparatus similar to that described previously. The TTF data are fit to the same empirical model previously used and median lifetimes are extrapolated at 85°C and rated voltage.

But the data collected from these capacitors differ in interesting ways from the data previously presented. Specifically, the distributions of failures in time display greater structure and complexity when compared with the data reported for the low-voltage tantalum polymer capacitors. The shapes of the TTF plots suggest the presence of more than one contributing degradation mechanism. These mechanisms are variously affected by changing voltage and temperature, with individual mechanisms being dominant at various voltages, temperatures, and times.

Representative data sets from 25V, 35V, and 50V devices are presented to convey the general nature of the collected data. Some educated guesses are made regarding what is going on inside the capacitors as they fail at various voltages, temperatures, and times, and some conclusions are drawn regarding the overall reliability one might expect from this new family of tantalum polymer capacitors.

Test Samples and Test Conditions

It was desired to explore a reasonably wide range of voltage ratings in this work. However, at the time the experimental plan was conceived, there were very few fixed designs in regular production and there was not always a "standard" design to copy for a given capacitance and rated voltage. For these reasons and the desire to limit unnecessary experimental variables, the test samples were created according to a simple plan: (1) start with a single tantalum anode design, (2) create dielectric with 3 thicknesses roughly consistent with finished part ratings of 25V, 35V, and 50V, and (3) perform a single polymerization process on all the anodes.

An obvious advantage of this strategy is that the number of variables to track is reduced to essentially one: dielectric thickness. But a disadvantage is that these designs probably will not precisely match final production designs which will likely employ tantalum powders of different surface area per gram, slightly different formation-to-rated voltage ratios, and small process variations intended to enhance performance in specific designs. That is, the results of these tests may not precisely match the performance of the final commercial product, but should be very similar.

The final experimental design for the investigation involved formation voltages of 70V, 100V, and 130V at 80°C for the capacitors called 25V, 35V, and 50V devices, respectively. The resulting capacitance values were roughly 22uF, 15uF, and 10uF.

The formation-to-rated voltage ratio is not constant, but the values are generally close to 2.8 to 1, with the “50V” devices lagging behind at 2.6 to 1. To be consistent with the usual practice of using a higher formation-to-rated ratio for higher rated voltage devices, the 50V parts should have been formed at 150V. But this choice would be inconsistent with using the same anode design for each rated voltage since the chosen tantalum powder particle size limits the maximum allowed formation voltage. Nevertheless, the final designs provide valuable information on the general impact of rated voltage on lifetest performance.

100 capacitors were tested at each set of test conditions (rated voltage, test voltage, and test temperature) and the resulting times-to-failure were detected and recorded with a computer-driven monitoring system. Failure is defined as blowing a 1 ampere fuse. The test temperatures were limited to 85°C, 105°C, and 125°C. As much as possible, the same test voltages were employed at each temperature for capacitors of given rated voltage to facilitate direct observation of acceleration due to temperature.

The range of test voltages was determined experimentally to discover test conditions that would generate some failures in a reasonable time (within a few hours) while not taking an impractical time to approach 100% failures (generally not more than 3000 hours). It was not always possible to meet both objectives simultaneously, and the test voltages that were finally chosen typically fell into a fairly narrow range and were substantially higher than rated voltage (e.g., $1.8V_r$ to $2.2V_r$ for the “35V” samples). When test voltages much lower than the bottom end of the chosen voltage range were attempted, there simply were no failures during the maximum allowed test period of 3000 hours, a fact that speaks well of the robustness of these capacitors.

A practical comment is in order here. Weibull grading of high-reliability MnO_2 military capacitors per MIL-PRF-55365 **depends** on generation of at least one failure within the first 2.25 hours of testing at 85°C using test voltages that cannot exceed 1.5 times rated voltage. Weibull grading as defined above would not be practical for the 35V tantalum polymer samples because none of the capacitors would fail in the first 2.25 hours of testing at $1.5V_r$ (an occasional early failure is finally observed when the test voltage is raised to $1.7V_r$ which represents 60% of the formation voltage – a very high voltage for a tantalum capacitor).

Typical Time-to-Failure Test Data

It is impractical in this paper to present and fully discuss all of the collected data because of their volume. Instead, representative samples of the data are presented and the larger trends are identified. The primary focus is on the 35V samples, but the raw data for the 50V and 25V capacitors are subsequently introduced and briefly discussed.

Figure 1 contains time-to-failure (TTF) data collected at 105°C and test voltages ranging from $1.8V_r$ to $2.2V_r$ for the samples formed at 100V and called 35V rated samples. There are several distinct patterns that can be identified in the resulting TTF distribution curves .

First, there are some initial failures at the start of the test and the number of these initial failures increases as the test voltage increases. The number of initial failures is close to zero for test voltages less than $1.8V_r$ ($0.63V_f$). Second, failures occur relatively gradually after the initial failures for a time period that depends on the test voltage, with longer times at lower test voltages. Third, the capacitors start to wear out and many failures occur in a relatively short period of time. Finally, for the voltages where the onset of wear-out takes a long time, eventually the capacitors stop wearing out and the TTF curve becomes more horizontal again. These regions of the TTF curves are identified in Figure 1.

Some observations regarding these characteristics are in order. First, the concentration of failures at roughly 0.02 hours occurs for a specific reason. The power supply voltage is ramped from 0V to the test voltage in 60 seconds, and the first failures do not occur until the voltage gets very close to the test voltage. This tends to concentrate the initial failures into a tight distribution.

If the test voltage could be applied instantly, the power supply could provide enough current to blow many 1 ampere fuses simultaneously, and the monitoring system could collect the failure information rapidly enough, it is likely that the horizontal portion of the TTF curves would extend to shorter times without significant overlap of the curves. But to accommodate the limits of the power supply and the rest of the test apparatus, a 60 second voltage ramp time was employed and it produced the best overall results.

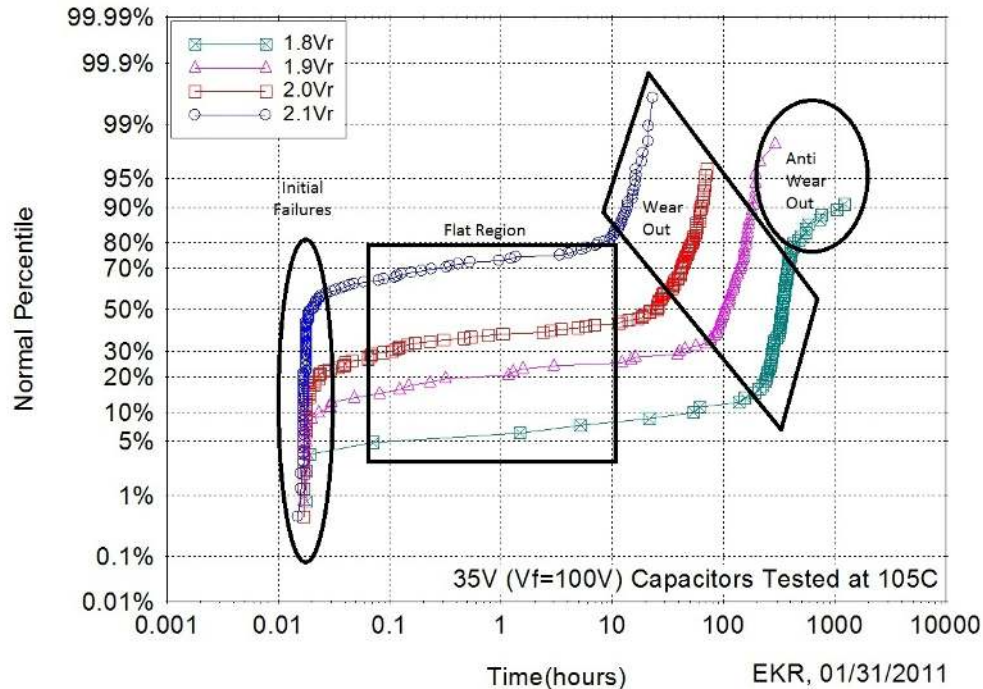


Figure 1. Lognormal Plot of Failure Percentile versus Time-to-Failure at 1.8V_r, 1.9V_r, 2.0V_r, and 2.1V_r, for Tests Performed at 105°C on 15µF, 35V Experimental Tantalum Polymer Capacitors.

The initial failures and flat part of each TTF distribution comprise a smaller percentage of the failures as the test voltage is substantially reduced (they are <15% at 1.8V_r). If the applied voltage had been rated voltage or lower, it is easy to project from the trend of the curves that this percentage approaches zero. Consequently, while interesting to observe and comment on, these regions of the failure distribution likely provide no practical information regarding reliability at or below rated voltage. For this reason they will be ignored during estimation of voltage and temperature acceleration factors in subsequently lifetime calculations, but they will receive mention when the potential underlying mechanisms are discussed.

Conversely, the near-vertical wear-out portion of the TTF distribution applies to an increasing percentage of the capacitors as the test voltage approaches rated voltage (it is ~68% at 1.8V_r). Consequently, this part of the failure distribution is of high interest as acceleration models are developed.

Finally, the portion of the TTF distribution that indicates cessation of wear out at long test times also applies to a larger percentage of the capacitors as the test voltage is falls (~20% at 1.8V_r). This region of the failure distribution might influence lifetime calculations if under certain circumstances no parts could fail because this mechanism became dominant before the onset of wear-out.

Voltage Acceleration Model

It is clear that the data of Figure 1 suggest that the wear-out regions of the TTF curves generated at 105°C are sensitive to the test voltage. That is, wear-out occurs at shorter test times as the applied voltage increases. Moreover, the relatively uniform spacing of the TTF curves – perhaps excluding the curve

generated at 2.1V -- suggests that wear-out can be effectively modeled as a power function of voltage. Such a model should allow reasonable extrapolation of wear-out behavior to voltages lower than the test voltages. (Of course all extrapolations are inherently risky, and other factors that could come into play at lower test voltages must be considered when evaluating the resulting predictions.)

For the purposes of this paper, the acceleration model is chosen to take the form of a power law:

$$A_v = \frac{t_1}{t_2} = \left(\frac{V_2}{V_1} \right)^\eta, \text{ where } A_v \text{ is the voltage acceleration factor and } \eta \text{ is an empirically-derived exponent.}$$

The value of η is determined by plotting the t_{50} times (or projected t_{50} times) of each TTF distribution on a log-log plot of t_{50} versus voltage and determining the slope of the resulting curve.

Further, t_{50} times for lower applied voltages can be extrapolated from the known data if a line having slope= η is extended to lower voltages on the aforementioned plot. An illustration of the strategy for processing the wear-out portion of the data of Figure 1, to find the voltage ratio exponent and extrapolate to lower voltages, appears in Figures 2 and 3. Note that when choosing where to place the parallel lines in Figure 2, an effort was made to find the portion of the TTF distribution that most accurately represents only the wear-out mechanism and avoids influence from other mechanisms.

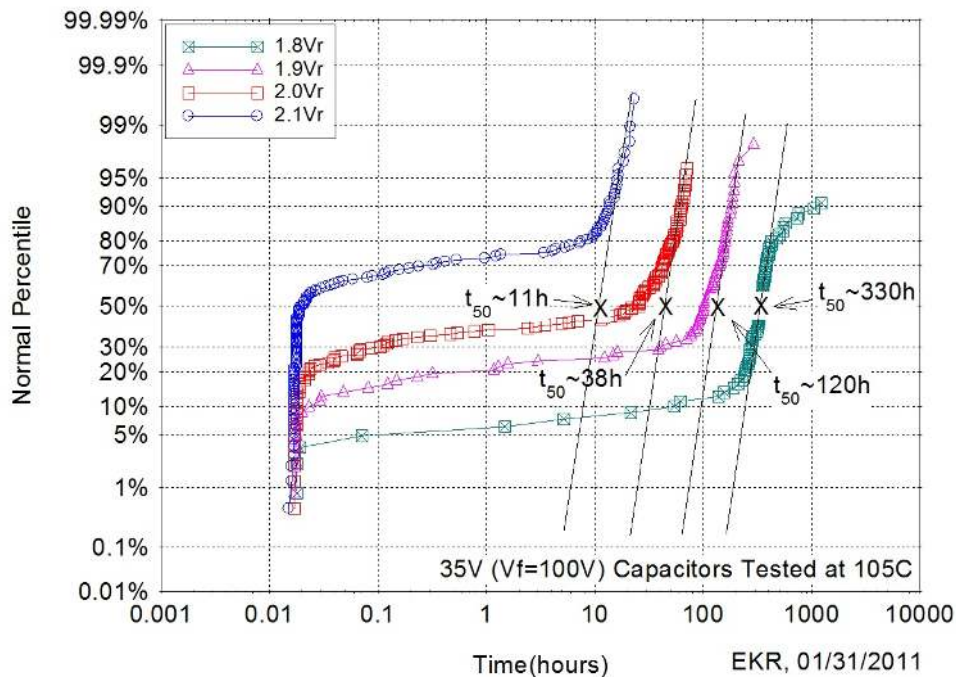


Figure 2. Estimates of t_{50} Times of the Wear-Out Phases of Time-to-Failure Plots for 35V Experimental Tantalum Polymer Capacitors Tested at 105°C and Voltages from 1.8 to 2.1Vr.

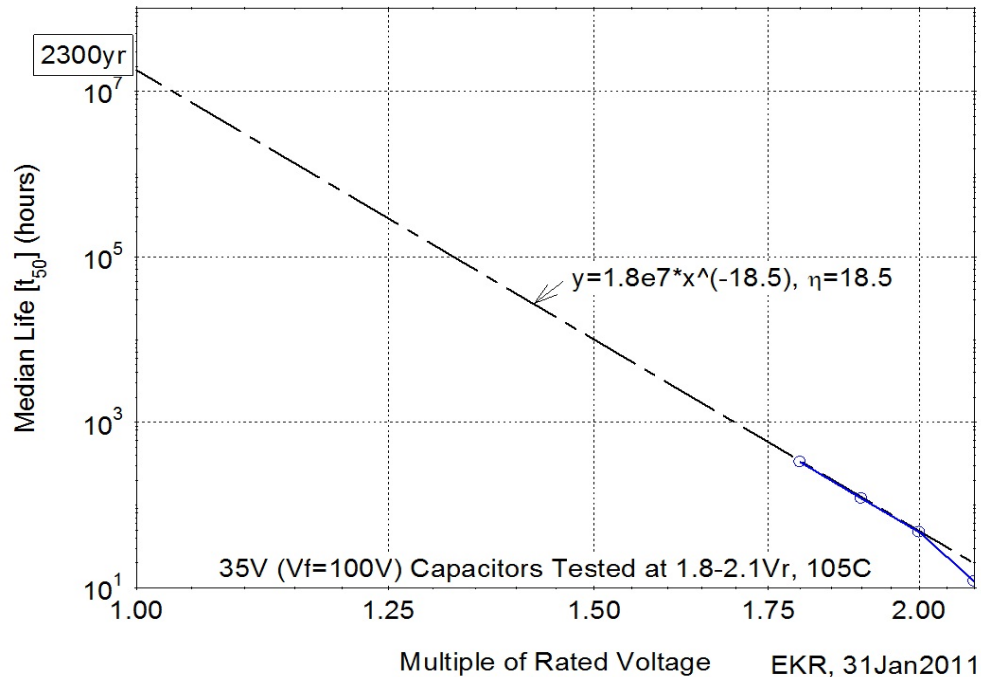


Figure 3. t_{50} Times versus Test Voltage, Calculation of Voltage Ratio Exponent η , and Extrapolation to Lower Test Voltages for 35V Experimental Tantalum Polymer Capacitors Tested at 105°C and Voltages from 1.8 to 2.1Vr.

This graphical method provides an estimate of $\eta=18.5$ for the voltage ratio exponent for the voltage acceleration model. For comparison, the work done on 6V tantalum polymer capacitors produced estimates of $\eta=14.5$ at 125°C, $\eta=16.5$ at 105°C, and $\eta=19.0$ at 85°C. While not identical, the η estimates for the 35V samples appear to be in the right neighborhood in spite of the limitations of the raw TTF data.

Observe that the data point at 2.1Vr does not fit the line in Figure 3. 2.1Vr is about 74% of the formation voltage. Such a high test voltage has been observed in the past to stimulate at least one additional failure mechanism. In this case it is thought that the reduced t_{50} life time at 2.1Vr results from the presence of a second degradation mechanism and this data point was excluded from the estimation of η for this reason.

It is clear that the estimate of voltage acceleration created by the method of Figures 2 and 3 is only approximate and is subject to some error. However, since it is impossible to execute the lifetests at low enough voltage to discover something closer to the truth (at least in this investigator's lifetime), the method described provides a useful means to make reasonable predictions in spite of the inherent limitations.

TTF data were also collected at 85°C and 125°C for the 35V capacitors and at all three temperatures for the 50V and 25V capacitors. The combined data appear in Figures 4, 5, and 6 for the 35V, 50V, and 25V capacitors, respectively. While difficult to sort out at first, the combined plots make it possible to discern how the influence of the active regions of the failure distributions (initial failures, flat region, wear-out region, and anti-wear-out region) varies with voltage and temperature.

The reader is asked to forgive the strange order of presentation of the data for the various rated voltages. The chosen order -- 35V, 50V, and then 25V -- is thought to aid the description of the data. That is, the 35V samples behave in the most orderly and easily described manner, followed by the 50V samples' data that behave a little oddly at the lower voltages at 85°C, and finally the 25V samples' data that might be hard to understand at all without seeing the 35V and 50V samples' data first.

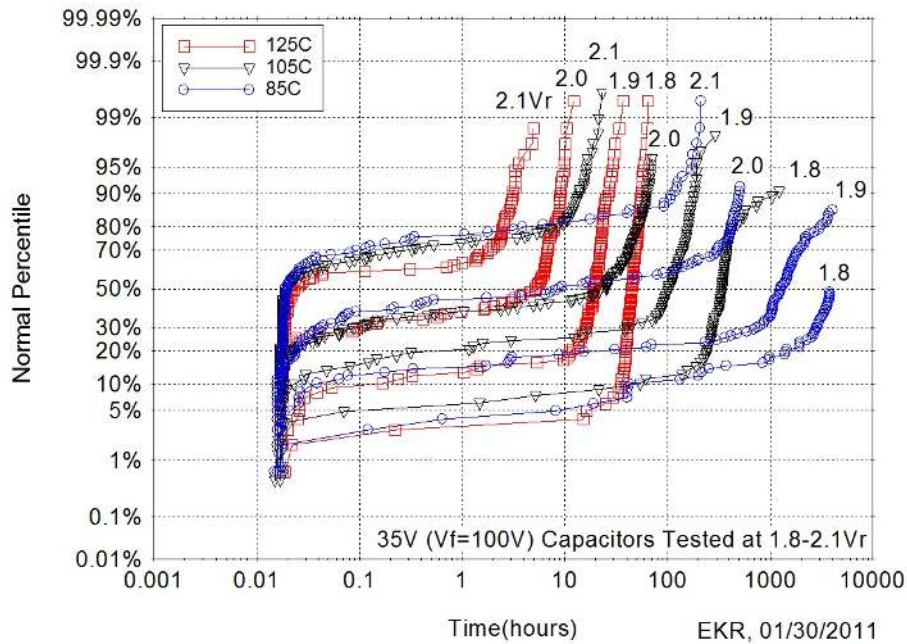


Figure 4. Lognormal Plot of Failure Percentile versus Time-to-Failure at $1.8V_r$, $1.9V_r$, $2.0V_r$, and $2.1V_r$ for Tests Performed at 85°C , 105°C , and 125°C on $15\mu\text{F}$, 35V Experimental Tantalum Polymer Capacitors.

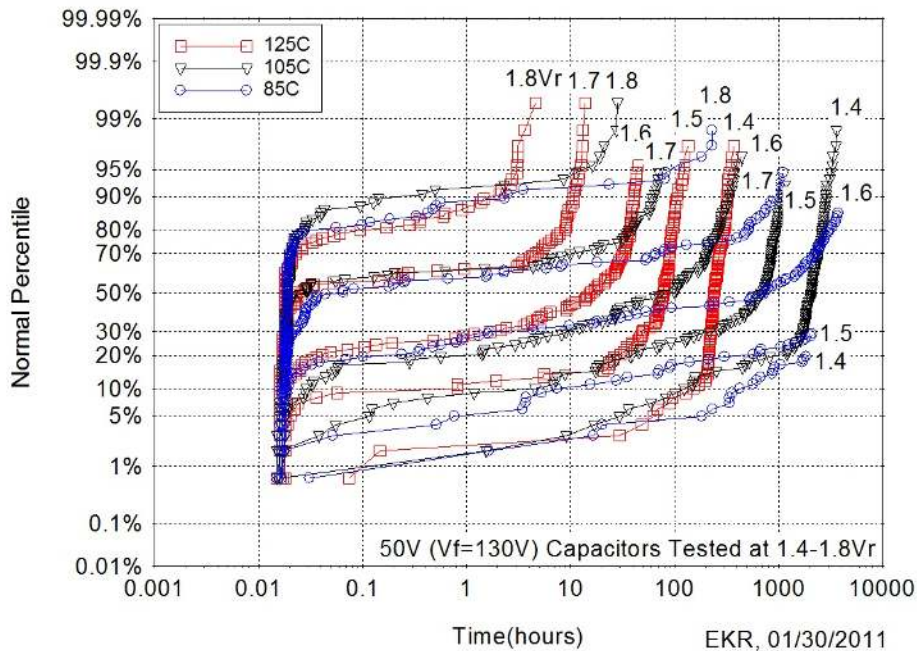


Figure 5. Lognormal Plot of Failure Percentile versus Time-to-Failure at $1.4V_r$, $1.5V_r$, $1.6V_r$, $1.7V_r$, and $1.8V_r$ for Tests Performed at 85°C , 105°C , and 125°C on $10\mu\text{F}$, 50V Experimental Tantalum Polymer Capacitors.

Observe in Figure 4 that the wear-out portion of the TTF distributions becomes more pronounced as temperature rises from 105°C to 125°C , but becomes muted as temperature falls to 85°C . Also observe that

the durations of the flat portions of the failure distributions become shorter at higher temperatures which means that the capacitors enter wear-out more quickly at higher temperatures. This pattern also exists in Figures 5 and 6 and will be quantified in the next section.

In contrast to the clear temperature sensitivity of the wear-out portions of the TTF distributions, observe that there is very little temperature sensitivity for the flat portions of the TTF distributions. In Figure 4 it appears that fewer parts fail in this region at 125°C than do at the lower temperatures, but half of the time more fail at 105°C than at 85°C.

After observing similar patterns in Figures 5 and 6, one concludes that there may generally be less tendency for failures at 125°C in the flat regions, but no clear pattern at 105°C and 85°C. This lack of clear temperature dependence is commented on subsequently when an attempt is made to describe the mechanisms at work in these regions of the TTF distributions.

Overall, it is clear that the flat portions of the TTF distributions are more highly dependent on the applied voltage rather than on the test temperature. But if the test voltage were sufficiently reduced below the levels represented in the plots, this part of the plots would disappear completely, leaving primarily the wear-out region (as is seen in the previous work done on 6V rated capacitors). Thus it is thought that the flat regions of the TTF distributions have little significance regarding the long-term reliability of these capacitors at more normal application voltages, and this behavior will not be quantitatively modeled here.

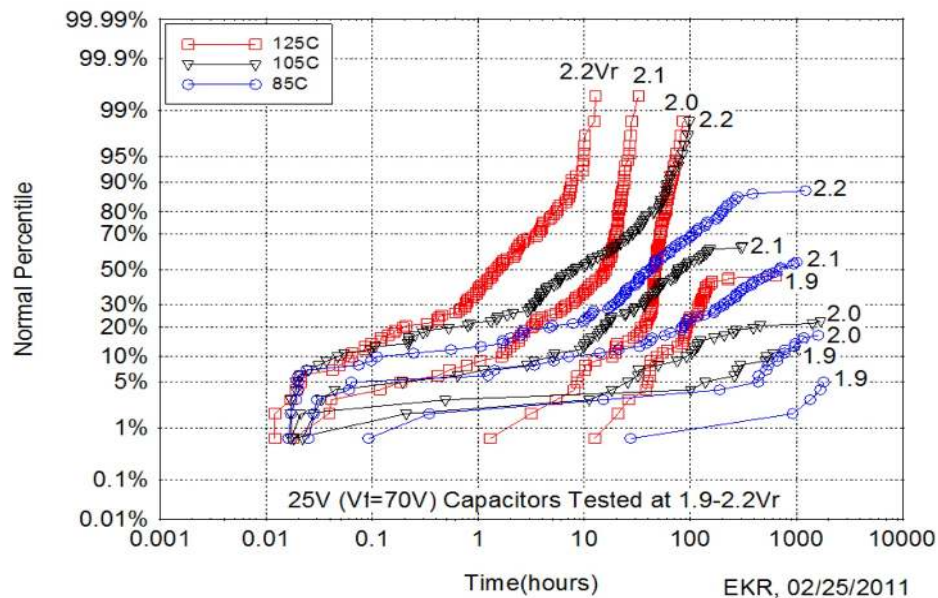


Figure 6. Lognormal Plot of Failure Percentile versus Time-to-Failure at 1.9V_r, 2.0V_r, 2.1V_r, and 2.2V_r for Tests Performed at 85°C, 105°C, and 125°C on 22μF, 25V Experimental Tantalum Polymer Capacitors.

The final region of the TTF distributions of Figures 4-6 that requires description is the region called here the anti-wear-out region. The 35V capacitors show very little of this behavior except for the 1.8V_r and 1.9V_r data at 105°C in Figure 4. But there is a general clockwise rotation of the wear-out part of the TTF distribution that reflects a general slowing-down of the failures in time at 85°C at the lower test voltages which delay failures until later times. It seems that this might reflect a mixing of the wear-out and anti-wear-out regions of the TTF distributions under certain test conditions.

This same pattern appears for the 50V parts in Figure 5 at 85°C and the lower test voltages, and very distinctively in Figure 6 for the 25V parts. Because the test voltages are so high in comparison to expected

application voltages, it is not presently known whether the anti-wear-out region has special significance in the estimation of long-term capacitor reliability or not. Further work must be done to better understand this behavior.

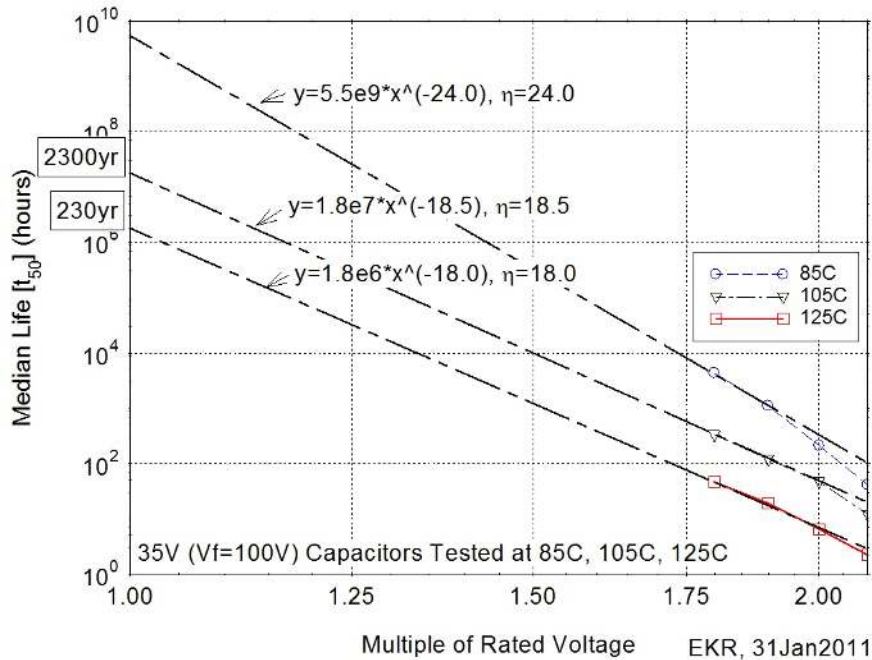


Figure 7. t_{50} Times versus Test Voltage, Calculation of Voltage Ratio Exponent η , and Extrapolation to Lower Test Voltages for 35V Experimental Tantalum Polymer Capacitors Tested at 85°C, 105°C, 125°C and Voltages from 1.8 to 2.1Vr.

Finally, to close out the subject of voltage acceleration of the wear-out region of the TTF distributions, plots of t_{50} versus test voltage, calculation of the voltage ratio exponent η , and extrapolation of expected t_{50} s at lower test voltages are performed using the data of Figure 4 at all three temperatures. The results are presented in Figure 7 for the 35V capacitors.

The estimate of η generated from the 125°C data is generally consistent with the estimate generated from the 105°C data. Also, the data point at 2.1Vr is closer to the line (but still omitted from the calculation). However at 85°C, substantial nonlinearity is evident in the data points. This provides additional evidence that there is more than one mechanism at work.

Even if one disregards the nonlinearity and other imperfections of the data, it is clear that the voltage acceleration exponent η is temperature dependent. Subsequently we learn that the activation energy E_a used in the Arrhenius model for temperature acceleration is voltage sensitive. This interaction of voltage and temperature was also observed in the earlier work with the 6V devices and was the motivation for exploring a physics-based model that simultaneously addressed voltage and temperature acceleration.

The physics-base model is inherently more elegant than the simple empirical model employed here. However its form and the determination of the appropriate constants become burdensome if one wants to accommodate the effects of multiple mechanisms in the data. For this reason, the simpler, but much less elegant empirical model was used in spite of its limitations.

Graphical analysis of the data for the 50V and 25V capacitors proceeds similarly as for the 35V capacitors, but is not shown here. These data are even more confounded by the interaction of the various regions of TTF distributions (i.e., the various degradation mechanisms) and do not add anything meaningful to the

discussion. However, they are generally consistent with the results for the 35V capacitors in regions where the mechanisms operate independently.

Temperature Acceleration Model

As discussed above, the TTF plots in the wear-out region of the failure distributions are sensitive to the test temperature. As is observed in Figures 4-6, capacitors wear out faster at higher temperatures and slower at low temperatures. As was the case for changing test voltage, the wear-out distributions are fairly uniformly spaced with temperature which suggests that temperature acceleration of the wear-out region of the TTF distribution can be predicted by a relatively simple formula.

In this study we use a simple Arrhenius model for temperature acceleration: $A_t = \frac{t_1}{t_2} = e^{\left[\frac{E_a}{k} \left(\frac{1}{T_1} - \frac{1}{T_2}\right)\right]}$, where

A_t is temperature acceleration of time, k is Boltzmann's constant (8.62E-5 eV/K), E_a is an empirically-derived activation energy, and T is absolute Kelvin temperature.

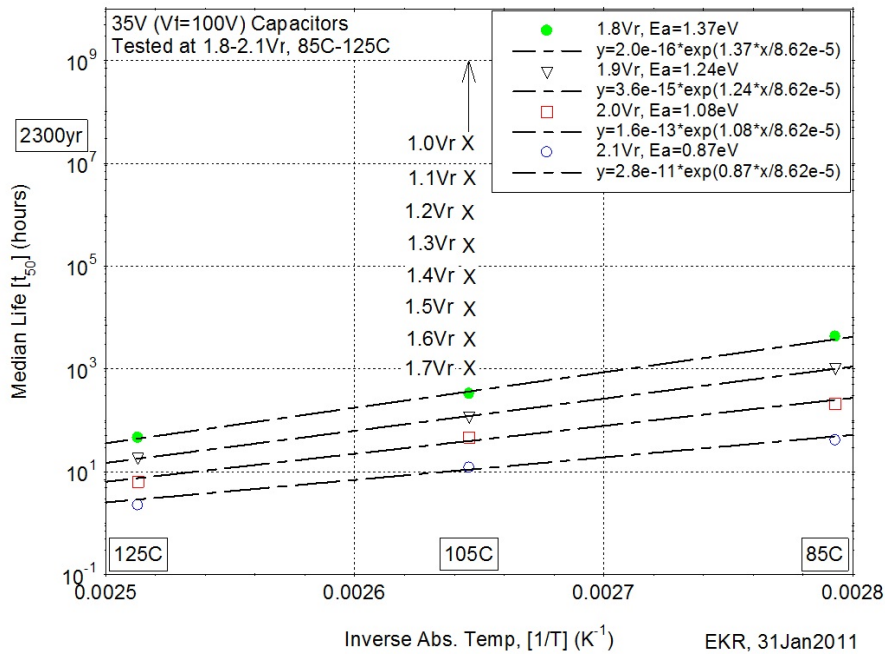


Figure 8. t_{50} Times versus Inverse Absolute Temperature, Calculation of E_a , and Extrapolation of Results to Lower Voltages for 35V Experimental Tantalum Polymer Capacitors Tested at 85°C, 105°C, and 125°C, and Voltages from 1.8 to 2.1Vr.

To determine the activation energy at each test voltage, the t_{50} time (or projected t_{50} time) of the wear-out region of each TTF distribution is plotted on graph of log-time versus inverse absolute temperature graph. Then the t_{50} times for a given test voltage and multiple test temperatures are connected with a best-fit line. The slope of this line provides the activation energy at the test voltage. The results of this exercise appear in Figure 8 where the equation of each best-fit line appears in the legend.

Observe that the activation energies are indeed sensitive to the test voltage, and increase as the applied voltage falls. This was also seen in the previous work with 6V tantalum polymer capacitors.

The activation energies in the present study range from a little less than 1.0eV to about 1.4eV at the lowest practical test voltage of 1.8Vr (lower voltages do not produce enough failures). In the previous work on 6V capacitors, test voltages that produced similar t50 times at 105°C ranged from 1.1eV to 1.4eV, so the present results for temperature acceleration of the wear-out region of the TTF distributions are generally consistent with the previous work.

A final exercise is performed in Figure 8 to extrapolate from the experimental data to lower test voltages. This extrapolation was done by placing X's on the graph above the fit lines with generally similar, but slightly increasing spacing at intervals of 0.1Vr. This is a guess regarding where the t50 times would have fallen had the test voltage been reduced at the test temperatures.

While obviously not a highly precise exercise, it is gratifying to see that the X at rated voltage and 105°C lands in the same general neighborhood (2300 years) as was predicted by extrapolation of the 105°C data on the voltage acceleration graph of Figure 7. Again, all extrapolations outside the range of the collected data are inherently risky, and other factors that could come into play at lower test voltages must be considered when evaluating the resulting predictions.

Mechanisms

It is clear that more than one mechanism is at work in the TTF distributions discussed in this paper. This is in striking contrast to the TTF distributions presented in the previous work concerning 6V tantalum polymer capacitors where the TTF distributions contained only one dominant mechanism, the wear-out mechanism.

To this point in the discussion the various mechanisms have not been identified, but rather they have been qualitatively described based on how they affect the appearance of various regions of the TTF distribution. The qualitative descriptions were (1) initial failure region, (2) flat region, (3) wear-out region, and (4) anti-wear-out region which refer to the shape of the TTF distribution from early time to later time.

Any meaningful discussion of the underlying mechanisms must reference our best understanding of the conduction physics of a tantalum polymer capacitor. Since PEDOT is a P-type semiconductor material, the tantalum polymer capacitor is an MIS (metal-insulator-semiconductor) device where tantalum is the metal, tantalum pentoxide is the insulator, and PEDOT is the semiconductor⁴.

MIS devices have conduction behavior that is principally governed by the energy levels found at the interface of the insulator and the semiconductor (work functions of the insulator and semiconductor plus any electric charge located at the interface). These energy levels provide a barrier to conduction when electric fields having direction consistent with the defined capacitor polarity are imposed on the insulator. If the applied field exceeds the barrier height, significant conduction occurs. If more than a small amount of conduction occurs at high electric field strength, significant heat is generated and dielectric breakdown can occur due to thermal runaway. The subsequent discussion of mechanisms will start with this foundation.

Freeman, et. al.⁴ describe the breakdown voltage behavior (BDV) of capacitors made entirely with in-situ polymerized PEDOT versus entirely with pre-polymerized PEDOT. For the “in-situ-only” capacitors, BDV increases with dielectric thickness and then saturates at about 40V, but for the “pre-poly-only” capacitors, breakdown voltage continues to rise with dielectric thickness.

They indicate that a likely reason for saturation of the BDV characteristic of the “in-situ-only” capacitors is charge at the interface that “pins” the potential barrier such that it cannot rise as the electric field applied to the insulator rises. This interfacial charge likely results from charge-bearing species left behind during the in-situ polymerization process.

In contrast, the pre-polymerized dispersion of PEDOT particles employed in the “pre-poly-only” capacitors does not contain any residual charge-bearing species since the chemical reactions are complete and any

residual charged particles are removed before the polymer dispersion is applied to the capacitor. In the presence of pristine dielectric and absence of charge to pin the potential barrier, the barrier is free to grow with applied electric field and BDV is free to rise with dielectric thickness without the saturation observed in the “in-situ-only” capacitors.

The tantalum polymer capacitors described in this work are a hybrid of the two extremes described above. That is, a few layers of in-situ PEDOT are deposited inside the tantalum anodes, thoroughly washed to remove as much charged residue as possible, and then covered with pre-polymerized PEDOT. It is reasonable to expect that the behavior of the potential barrier in these devices will fall somewhere between the two extremes described above.

The initial failures are almost certainly devices whose breakdown voltage is exceeded as the voltage is ramped up to the final test voltage during the first 60 seconds of the test. Due to the hybrid nature of the polymer cathode, it is not surprising that there is considerable spread in the observed breakdown voltages (demonstrated by the non-vertical slope of the initial failure region of the TTF distribution), and that more capacitors fail in this initial failure region as the test voltage rises.

For capacitors that survive the initial voltage ramp (analogous to a BDV test performed in 60 seconds), it is hypothesized that a few more capacitors fail over time as the potential barrier in the surviving capacitors deteriorates slowly with time, perhaps because of accumulation of trace mobile negative charge at the interface.

This hypothesis is based on the assumption that the flat region in the TTF distributions is consistent with behavior of the barrier. This assumption is supported by the very low temperature sensitivity of failures in this region and the fact that the barrier height and related electronic conduction is found to be largely independent of temperature⁴.

It is hypothesized that the wear-out region of the TTF distributions is caused by increased electric field in the insulator as more oxygen is stolen from the dielectric in the neighborhood of the interface of the tantalum and the dielectric. As oxygen is stolen from the dielectric near the tantalum metal, the dielectric there becomes more conductive. Growing conductivity of the dielectric near the metal causes the effective thickness of the remaining good dielectric to fall and the electric field strength to rise. Given enough time, the electric field grows to the point where the potential barrier can no longer contain it and dielectric breakdown occurs.

Oxygen vacancy generation, migration, and absorption into the tantalum metal occur naturally over time and are significantly accelerated by temperature and the electric field. This degradation mechanism was identified as the likely cause of wear-out in the previous investigations of low-voltage tantalum polymer capacitors referred to above.^{2,3}

The remaining region of the TTF distributions is the anti-wear-out region where wear-out appears to slow down or stop. It is hypothesized that with sufficient voltage, time, and temperature, de-doping of the polymer occurs at the interface of the polymer and the dielectric. This process produces new insulator (de-doped polymer) at the interface which reduces the electric field strength in the original dielectric, counteracting the increasing field from oxygen vacancy generation.

Some support for this hypothesis comes from the observation that BDV in “pre-poly-only” capacitors sometimes exceeds the original formation voltage of the dielectric when the voltage is ramped up slowly. Subsequent measurement of devices that were exposed to very high voltage, but did not break down, shows reduced capacitance that is explained by introduction of additional insulation (de-doped polymer) between the original dielectric and the remaining conductive polymer layer. If this hypothesis is valid, it is not known whether this mechanism has any relevance to long-term life predictions at more normal operating conditions.

Summary and Conclusions

A brief history of tantalum capacitors shows that the use of conductive polymer as a replacement for MnO₂ as the cathode layer was primarily driven by the need for lower ESR. But it was soon discovered that the reliability of these tantalum polymer capacitors was quite good, often rivaling and sometimes exceeding that of MnO₂ capacitors. However, the range of rated voltages initially available was limited because good reliability was not possible at the higher rated voltages.

With the introduction of pre-polymerized PEDOT polymer dispersions, the existing voltage limit for tantalum polymer capacitors is breached and reliable tantalum polymer capacitors with voltage ratings of 25V and higher can now be manufactured.

The natural need to assess the long-term reliability of these higher rated voltage devices lead to the present reliability investigation. Here, highly accelerated lifetesting is employed to establish voltage and temperature acceleration models and predict life at more normal application conditions.

TTF failure distributions were collected on carefully prepared experimental capacitor designs at various voltages and temperatures. The resulting failure distributions are found to contain identifiable regions that likely correspond with separate degradation processes. These processes or failure mechanisms are found to be dominant at different times during the test. Moreover they are variously affected by voltage and temperature, providing clues regarding the underlying physics.

The wear-out regions of the TTF distributions were deemed to be of primary importance since the other mechanisms are thought to either disappear or not impact dielectric failure under normal application conditions. So, the behavior of the wear-out regions of the TTF distributions were graphically analyzed and the results fit to simple empirical voltage and temperature acceleration models.

The resulting models predict very long life (median life beyond 1000 years) under normal application conditions. Even discounting for early failures and process variation, it is clear that these capacitors have sufficient reliability for all routine, and many high-reliability applications. They may even be more reliable than their lower-voltage siblings.

The paper ends with discussion of the various likely failure mechanisms and their underlying physics. Understanding of these complex devices is still in its infancy, but much of the observed electrical behavior can be understood if one accepts that these capacitors are MIS structures and behave according to MIS theory.

References

¹ E. Reed and J. Marshall, "18 Milliohms and Falling – New Ultra-Low ESR Tantalum Chip Capacitors," CARTS '99 Proceedings of the 19th Capacitor and Resistor Technology Symposium, p. 133 (1999).

² J. Paulsen, E. Reed, and J. Kelly, "Reliability of Tantalum Polymer Capacitors," CARTS'04 Proceedings of the 24th Capacitor and Resistor Technology Symposium, p. 114 (2004).

³ E. Reed, J. Kelly, and J. Paulsen, "Reliability of Low-Voltage Tantalum Polymer Capacitors," CARTS USA 2005 Proceedings of the 25th Symposium for Passive Components, p. 189 (2005).

⁴ Y. Freeman, W. Harrell, I. Luzinov, B. Holman, and P. Lessner, "Electrical Characterization of Tantalum Capacitors with Poly(3,4-ethylenedioxythiophene) Counter Electrodes," Journal of the Electrochemical Society, p. G65 (2009).